30th Congress of the International Council of the Aeronautical Sciences
DCC, Daejeon, Korea ; September 25-30, 2016

BOUNDARY LAYER STATE INFLUENCE ON START OF THE INWARD-TURNING INTAKE

N.V. Voevodenko*, A.A. Gubanov*, D.Yu. Gusev*, M.A. Ivankin*, D.S. Ivanyushkin*, V.Yu. Lunin*, P.A. Meshennikov*, Yu.G. Shvalev*, V.A. Talyzin* and V.A. Yakovleva*
*Central Aerohydrodynamic Institute named after Professor N.E. Zhukovsky (TsAGI), Russian Federation

Keywords: *hypersonic vehicle, aerodynamics, scramjet propulsion, CFD, experiments*

Abstract

CFD and EFD studies of the flow in the air intake device of the high-speed civil aircraft model HEXAFLY-INT have been performed.
It was shown that the characteristic feature of this intake is the occurrence of subsonic separation zone in the central part of flow.
Boundary layer on the intake compression surface influences essentially on the development of the separation zone downstream. The turbulent boundary layer in this case is more preferable than laminar one. Right selection of the turbulence generators makes it possible to improve substantially the intake characteristics.

1 Introduction

The right selection of the air intake parameters of is one of the key moments in the aerodynamic design of high-speed aircraft with air-breathing jet engine. This paper presents the results of numerical and experimental studies of flow in the inlet area of the air intake model of the high-speed experimental flight test vehicle (EFTV). This work was performed within the 'High Speed Experimental Fly Vehicles - International' (HEXAFLY-INT) project with partners from Europe, Russian Federation and Australia.

The shape and geometry of the air intake considered in this paper was developed earlier as part of the EU LAPCAT / HEXAFLY and LAPCAT II projects. Within the HEXAFLY-INT Project such intake was investigated only by the Russian partners. The concept, basic ideas and the results of work on creation of the EFTV air intake are stated in [1-4]. The concept of considered air intake is based on popular idea for the design of the air intakes of hypersonic propulsion systems along streamline tracing of the converging conical flow [5]. The shape of the intake configuration is hereby defined by streamlines and stream surfaces from an inviscid template flow field. Appropriate corrections to the presence of the boundary layer, i.e. local displacement thickness, are subsequently applied to the inviscid design. For most practical applications this method is quite effective, but it neglects secondary effects such as the occurrence of local separation bubbles or cross-flow phenomena which can lead to significant degradation of the overall intake performance up to the intake unstart.

A detailed study of the occurrence of cross flow phenomena within the intake boundary layer and the entropy layer in the convergent flow, which is formed in the intake of LAPCAT/HEXAFLY scramjet configuration, is presented in [6]. This paper shows that the main cause of the cross-flow (side deflection of the airstream) are inviscid phenomena. Their main sources are blunted sweep leading edge in conjunction with swept inclined surface. A basic mechanism of the cross-flow occurrence is associated with the interaction of oblique shock waves among themselves and with the entropy and boundary layers. Since the cross-flows were not taken into account during the design process, it leads to the accumulation of decelerated fluid pockets in the vicinity of the combustor entrance. This effect could result in an earlier unstart with respect to the ideal intake.

Despite the fact that the main mechanism of the cross-flows and of the separation zones is inviscid, the further development of the resulting separation zones downstream highly depends on the state of the boundary layer on the intake compression surface. So, this paper focuses on the influence of the boundary layer state on the intake performances. Numerical simulations and tests in the TsAGI's wind tunnel T-116 have been performed for the EFTV HEXAFLY-INT intake model.

It was shown that when the boundary layer on the intake compression surface is laminar, the deceleration flow in the central part leads to the forming of the large separation zone. This zone covers a most part of the engine duct entrance section and leads to the air intake unstart. If the boundary layer on the intake compression surface is turbulent, the separation zone is substantially smaller, and the intake starts for most regimes of interest.

2 Intake geometry

EFTV propelled model geometry shown in Fig. 1, is a version of the experimental vehicle developed under LAPCAT-MR2 program as a conceptual design of hypersonic passenger aircraft to cruise at Mach 8 with an overhead inverted air intake. The bottom surface of the vehicle has a form of waverider, designed for cruising Mach number = 7 ÷ 8.

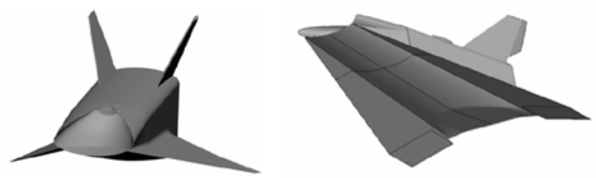

Fig. 1. Overall view of EFTV HEXAFLY-INT propelled model.

The flow patten in the intake is shown schematically in Fig. 2 (left picture). The leading and the closing shock waves, isentropic compression waves and the entrance to the combustion chamber are shown in red, blue and green, respectively. The streamlines are shown by dashed lines. The black solid lines indicate the flow boundary. The resultant compression surface is shown in blue on the right part of Fig. 2. It is determined by a number of streamlines emanating downstream from the compression surface. The front boundary of this surface is determined by the intersection of the stream surface with the initial shock wave. In order to smoothly integrate the intake compression surface in the aerodynamic shape of the entire aircraft, the insert was added, which is shown in red on the right picture of Fig. 2. It is oriented parallel to the free stream to minimize the flow disturbances. The resulting elliptical shape of the intake leading edge was then directly used to construct the external waverider airframe.

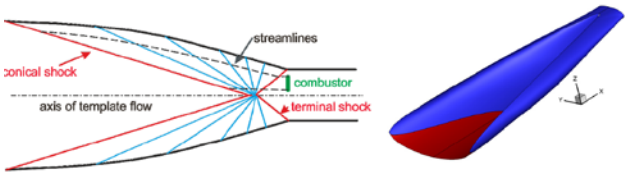

Fig. 2. Left – schematic illustration of the idea of the EFTV HEXAFLY-INT intake design. Right – the intake shape, red surface is the insert.

Corresponding corrections to the boundary layer, i.e., local displacement thickness is then applied to the inviscid form. For many practical applications this technique is quite effective, but it does not count the secondary effects such as the local separated areas occurrence and cross-flow phenomena, which may lead to significant degradation of the intake performances.

A detailed study of the cross-flow appearance and of phenomena in the boundary layer and the entropy layer in the convergent stream, which is formed in the intake under consideration, is presented in [6]. This paper shows that the main cause of the cross-flows are inviscid effects. Their main sources are sweep blunted leading edge in conjunction with swept inclined surface. A basic mechanism of the cross-flows occurrence is associated with the interaction of oblique shock waves among themselves and with the entropy and boundary layers.

In [6] it is also pointed out that the cross-flows lead to the development of a pocket of decelerated fluid along the intake symmetry plane near the engine duct inlet and the combustion chamber. This fact may lead to the earlier intake unstart.

Although the main mechanism of the cross flow and of the decelerated zone is inviscid, further development of the separation zones downstream strongly depends on the state of the boundary layer (BL) on the intake compression surface, i.e. it is laminar or turbulent.

Preliminary EFTV calculations and testing of its model in the TsAGI wind tunnel T-116 have shown that when the intake compression surface is flown with laminar boundary layer, the decelerated flow occurs in the central intake part and leads to the formation of large separation zone. This zone covers most of the engine duct input section and leads to the air intake unstart. If the boundary layer on the intake compression surface is turbulent, the separation zone is substantially smaller and the intake starts for most regimes of interest.

The final form of the HEXAFLY-INT propelled configuration model nose part is shown in Fig. 3. When choosing strategies and methods of calculation of this configuration it is necessary to take into account the peculiarities of the flow in this intake and be especially attentive to the separated zone of subsonic flow.

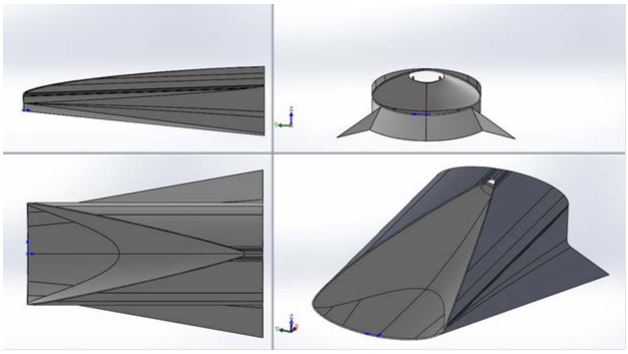

Fig. 3. The 3-D model of the HEXAFLY-INT EFTV air intake.

3 Intake studies methods

The HEXAFLY intake flow had been studied both by numerical simulation and by experiment in TsAGI's T-116 wind tunnel.

3.1 CFD tools

CFD studies of the air intake model were performed using the commercial software packages FLUENT and NUMECA.

Numerical simulation was based on the solutions of Reynolds Averaged Navier - Stokes (RANS) equations, closed by the Spalart-Allmaras (SA) turbulence model, which provides sufficient accuracy and stability of a solution. The free stream parameters correspond to the flow conditions adopted in the TsAGI's wind tunnel T-116.

The computational domain dimensions are selected on the basis of the bow shock wave location on the main design mode ($M_\infty = 7$). The free-stream flow conditions (static pressure, temperature, Mach number and angle of attack) were set on external boundaries of the calculation area. The no-slip and zero heat transfer conditions were set on the body solid surfaces.

The complexity of the intake configuration required high-resolution computational grids. Grids, used for numerical simulation by FLUENT and NUMECA packages, are shown in Fig. 4 and 5, respectively.

Numerical simulation by the FLUENT package was conducted in the range of Mach numbers $M_\infty = 5 \div 8$ and angle of attack $\alpha = -2° \div 8°$. The Reynolds number was calculated on the airframe body length and corresponded to the values: $Re_L = 6.88 \cdot 10^6$ at $M_\infty = 5$, $Re_L = 5.38 \cdot 10^6$ at $M_\infty = 6$, $Re_L = 7.66 \cdot 10^6$, $Re_L = 7.33 \cdot 10^6$ at $M_\infty = 7$ and $Re_L = 5.92 \cdot 10^6$ at $M_\infty = 8$.

The computational grid size in the air intake domain was approximately 8,000,000 units. When forming the grid for the nose part, about 80% of the cells were concentrated in the vicinity of the intake braking stages for more detailed flow pattern in this area (Fig. 4).

The implicit method of solution with an increasing Courant number was used. From 15 000 to 20 000 iterations were carried out to achieve the convergence and obtain the stationary steady solution.

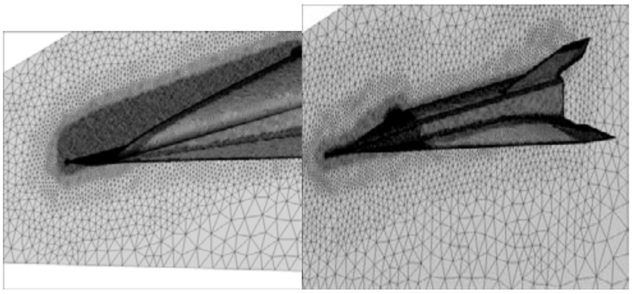

Fig. 4. Numerical grid for FLUENT.

To improve the reliability of the results similar calculations were also carried out with the help of other commercial software package NUMECA FINE / Open within the RANS equations.

Computational grid (Fig. 5) was generated in the semi-automatic mode. Mesh type is

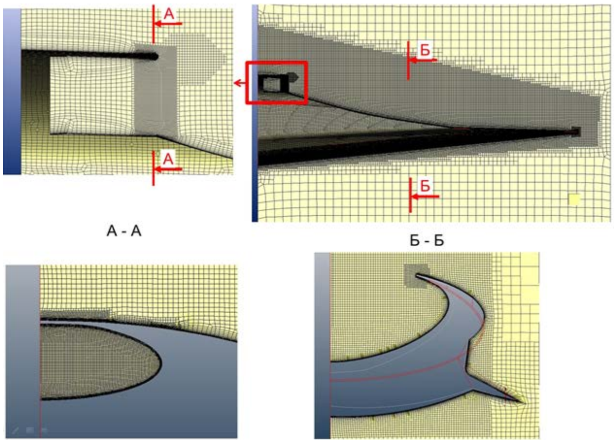

Fig. 5. Numerical grid for NUMECA.

hexahedral unstructured (Cartesian), with prismatic boundary layer. Calculations were carried out on grids with the cells number up to $12 \cdot 10^6$.

3.2 Experimental tool

Experimental studies of the EFTV HEXAFLY-INT model were conducted in TsAGI's wind tunnel T-116. The EFTV model installed in the T-116 test section is shown on Fig. 6.

The T-116 wind tunnel (WT) have the squared test section of 2.35m×1m×1m size and allows to carry out a wide variety of aerodynamic research of the aircraft models and of their components at super- and hypersonic flow velocities. The Mach number in the WT tests section varies from M=1.8 up to M=10. The unit Reynolds number Re variation range (referred to model length of 1m) is from $2.5 \cdot 10^6$ up to $42 \cdot 10^6$. These data correspond to modeled full-scale Re-numbers for 15 – 40 km height for flying vehicles (for characteristic vehicle length L=6 m). The T-116 Test Facility is a blow-down WT of ejector type with exhaust into atmosphere, with a variable supersonic diffuser and three-staged ejector. The tunnel is powered by pressure tank; the air is exhausted into atmosphere. The WT is equipped with electric heaters in order to prevent the air condensation in the test section.

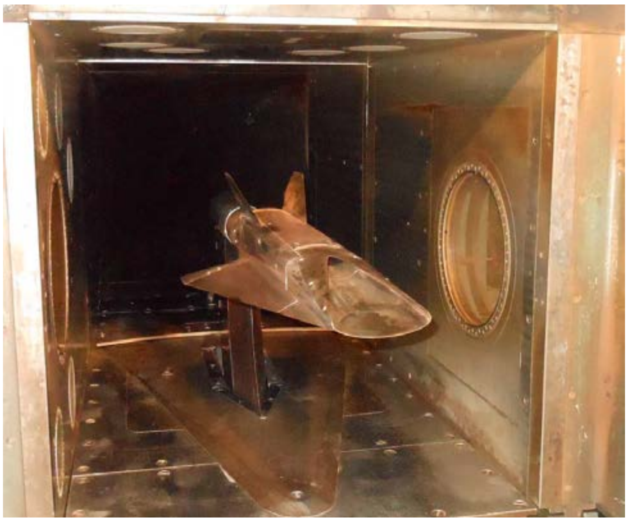

Fig. 6. EFTV model in the T-116 test section.

T-116 is a unique facility, it is super- and hypersonic WT of continuously working regime (test duration up to 7 minutes). It makes possible to obtain the steady-state flow pattern, and so, the results obtained correspond to the flight conditions more adequately, than those obtained in short-run WTs. This enables more proper link between wind tunnel and flight experiments and improves the understanding of the relevant flow physics and to further validate and improve the applied CFD tools.

4 Results

4.1 1st calculation stage results

1st series of numerical simulations have been performed for the nose part of the EFTV in Mach number range M_∞=5÷8 and angles of attack (AoA) α=-4°÷8°. It is important to underline that on this stage the boundary layer flow is presumed to be totally turbulent. CFD solutions were obtained for RANS equations with SA turbulence model. Re-numbers determined for fuselage length varied in range Re=$5.38 \div 7.66 \cdot 10^6$. Numerical tools, used for simulations, are described in 3.1.

The numerical simulation results are shown in Fig. 7-11. Fig. 7 shows the Mach number fields obtained by FLUENT package in the symmetry plane and in the inlet cross-

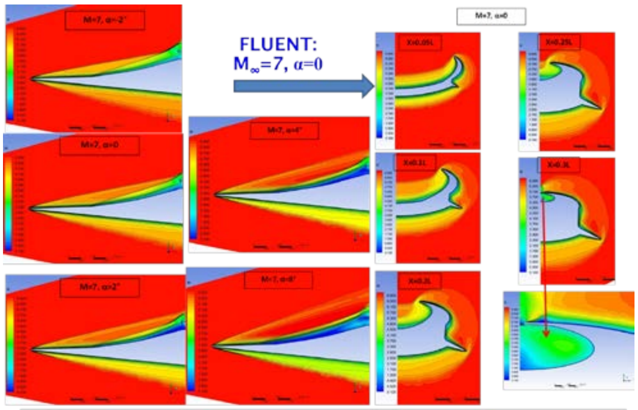

Fig. 7. FLUENT results: Mach number fields in the intake symmetry plane, M_∞=7, α=-2° to 8° and cross-sections, M_∞=7, α=0.

sections at a distances of X= 0.05 L_{ref}, 0.1 L_{ref}, 0.2 L_{ref}, 0.25 L_{ref} and 0.3 L_{ref} from the leading edge. Fig. 6 presents the FLUENT results for M_∞=7. Like in [6], the flow fields analysis showed that main peculiarity of this air intake is the presence of a significant subsonic zone (blue zones on the pictures), which is forming in the air intake central part as a result of boundary layer separation almost on all flow regimes.

Fig. 8 presents the longitudinal sections of the Mach number fields in the intake symmetry plane at free stream M_∞=5, 6 and 7 and α = -2°, 0 and 2°. As shown in Fig. 8, at M_∞=5 subsonic flow in central area is the most evident and is formed at a distance of approximately 0.1 L_{ref} from the leading edge and extends downstream up to the intake entrance. The AoA changing does not practically effect on the flow nature in the vicinity of braking steps and on the subsonic region size. The Mach number increase to M_∞=6 alters significantly the flow pattern at α=-2° and 0. When α=-2° subsonic zone is almost absent, and when α=0 it begins to form directly in front of the duct entrance. The

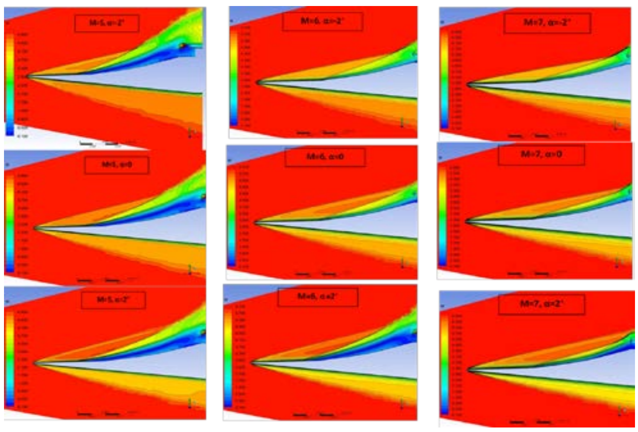

Fig. 8. FLUENT results: Mach number fields in the intake symmetry plane, M_∞=5,6,7, α=-2°, 0°, 2°.

transition to positive angles of attack leads to a sharp rebuilding of flow and a substantial expansion of the subsonic region. At Mach M_∞= 7 and 8, we observe a stabilization of flow in the vicinity of the compression surface, with a gradual increase in subsonic region with increasing angle of attack.

Results of similar calculations using the package NUMECA are shown in Fig. 9. At M_∞=7, we obtained the flow pattern, which has a structure close to that, obtained by FLUENT. In general, we observed good agreement between the calculations results of both numerical tools. Differences in pressure are

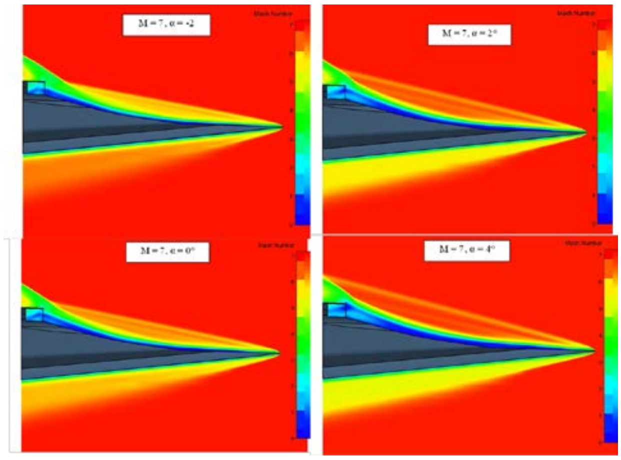

Fig. 9. NUMECA results: Mach number fields in the intake symmetry plane, M_∞=7, α=-2°, 0°, 2°.

observed at α = 4 ° in front of the inlet section.

A comparison of the flow parameters in the inlet section, received by two different codes is shown in Fig. 10 and 11. The results indicate a good agreement for basic parameters: air flow coefficient f, the density ρ, the pressure P and the Mach number.

Fig. 10 shows the field of Mach numbers in the plane of the intake entrance, obtained

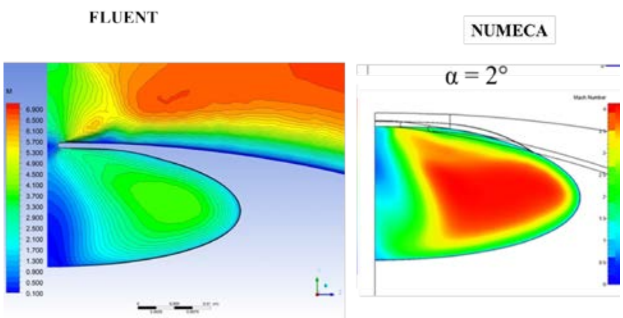

Fig. 10. Comparison of FLUENT and NUMECA results: Mach number fields in the intake entrance plane, M_∞=7, α=2°.

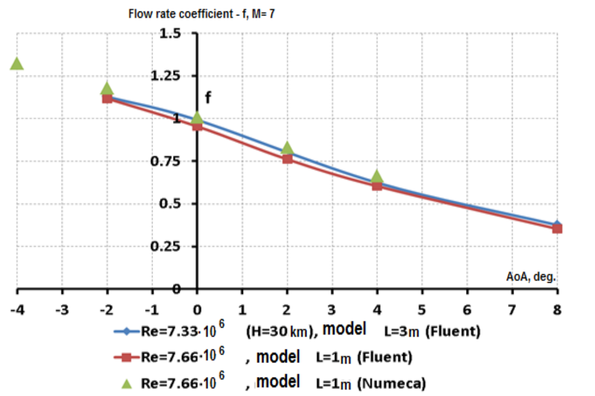

Fig. 11. Comparison of FLUENT and NUMECA results: the intake flow coefficient - f, M_∞=7.

using FLUENT and NUMECA packages at M_∞=7 and α = 2°. It can be seen, that different numerical tools gave similar results: a similar flow pattern and values of the local Mach numbers. Comparison of the calculations results for the flow coefficients at M_∞=7 and α = -2°÷8° is shown in Fig. 11. It should also be noted that the different numerical methods gave similar results. For Mach numbers M_∞= 7 and 8 the flow rate coefficient decreases monotonically with AoA increase (like Fig. 11). It is important to note that when α = 0 and Mach numbers M_∞= 7, 8 the flow coefficient takes values close to 1, according to the results of both software packages FLUENT and NUMECA. At Mach M_∞= 6 there is a sharp decrease in the flow rate in the range of α = 0°÷2°, which is caused by the abrupt flow rebuilding which form a large subsonic zone and leads to the intake unstart. Averaged Mach number and density ρ depend similar on the angle of attack.

Thus, the turbulent numerical simulations of the flows based on RANS-solutions with the SA turbulence model, has shown generally stable and regular flow in the air intake area. Besides we obtained high flow rate coefficients throughout the considered range of Mach numbers M_∞= 7 and 8 and angles of attack α =-4°÷8°. The boundary layer was assumed fully turbulent, and the Reynolds number, calculated over the length of the model fuselage is assumed to be Re=5.38÷7.66 · 10^6. We obtained close values of the flow coefficients by different software packages: FLUENT and NUMECA, which increases the reliability of the results.

4.2 Results of 1st tests in T-116

First series of the EFTV HEXAFLY-INT model tests was performed in September of 2014. Photo of T-116 tests section with EFTV HEXAFLY-INT model installed in it is shown in Fig. 6. This model is designed for the study of external aerodynamic characteristics and is made on a scale of 0.35 with respect to full-scale geometric parameters of the flight EFTV model, having a length of 2.876 m. The total area of the WT model plan projection is 0.2989 m^2.

Tests were conducted at the incident flow Mach M_∞=6 ÷ 8, and Reynolds number $Re_{L=1\ M}$= 5.92*10^6 ÷ 7.66 ·10^6, in the range of angles of attack α = -6 ÷ 12°, at a zero slip angle. At Mach number 8 the model aerodynamic characteristics are determined at slip angle β = 4°. The flaps effectiveness was investigated at Mach 7 in the range of deviation in the pitch channel δ = ± 6°, -12° and -18°, and in the roll channel δ = -6°.

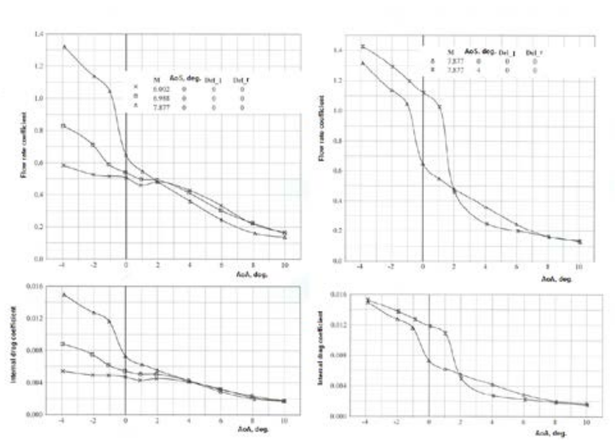

Fig. 12. Intake mass flow coefficient and internal drag coefficient of the EFTV model, T-116 test results.

Fig. 12 shows the dependence of the flow coefficient - f and of the internal drag coefficient - $C_{x\ int}$ on the model AoA=α at zero slip angle β at Mach studied. EFTV model was tested with expanded throat version (Fg=0.000696 m^2) compared with the standard (Fg=0.000595 m^2). Despite this, high flow coefficient f, indicating the intake start, was obtained only at Mach number M=8 for negative angles of attack α <-1°.

The boundary layer transition point study at an angle of attack α=0 and at Mach numbers

M = 6.0; 6.99 and 7.88 show that the lower surface of EFTV model is flown by a laminar boundary layer at all Mach numbers. At the entrance to the air intake when the number M = 7.88 flow also has a laminar boundary layer, but at Mach numbers of M = 6.0 and 6.99 we observed the transition region after laminar layer.

4.3 Comparison of 1st series of CFD computations and tests in T-116

Hereby, experimental research in TsAGI's wind tunnel T-116 gave quite different results, namely, flow coefficient is smaller than 0.6, it means the air intake unstarts at M_∞=6, 7, α =-4°÷8° and M_∞=8, α=0÷8°. Flow coefficients greater than 1, and clearly indicating the air intake start, are obtained only when M_∞=8, α=-4°÷-1°.

This fundamental difference between calculations and experimental data, points to the fact that the numerical simulation of the flow physics in the intake entrance area, when assuming turbulent flow in this case is wrong. Presumably, the boundary layer on the studied regimes is laminar and therefore less stable.

The main factor determining the physical picture of the flow in the intake entrance area is the relative position of the point of the boundary layer laminar-turbulent transition on the compression surface and of the boundary layer separation point. If the point of the laminar-turbulent transition is located upstream than the separation point, then the turbulent boundary layer develops on the compression surface, it leads to large dissipation of the internal flow energy, and results in the separation delaying and its weakening.

As shown in Fig. 7-9, the flow separation is mainly formed by the shock wave caused by the compression surface angle. If laminar boundary layer comes to the breaking point, then a more powerful separation is formed, and it extends downstream and covers the entire intake entrance cross section. The assumption of the laminar flow character is confirmed by studies of the boundary layer transition point in the T-116 (see. 4.2).

Forced determination of the turbulent boundary layer for numerical simulation on the entire intake compression surface makes the flow on it more stable, but it does not reflect the real physical picture of the flow. So, in this case, numerical simulation within the RANS equations with turbulent boundary layer does not simulate right real flow picture in the intake area.

At high Mach numbers (M_∞= 8) and negative angles of attack, external flow presses the boundary layer to the compression surface and does not allow it to separate, providing normal intake operation.

The results of 1st series of numerical and experimental studies have been published in paper [7]. In this paper it is also suggested that the main reason of CFD and EFD results difference is the boundary layer state: turbulent in CFD and laminar in EFD.

4.4 2nd CFD series

To verify the assumptions made above, we have repeated the calculations using FLUENT and NUMECA packages at M_∞=7 and α=0° with pre-determined laminar boundary layer. When performing the calculations, both software packages met the problems with the solutions convergence. After all we have managed to get the solution convergence and we obtained the flow coefficient of about 0.5. However, apparently, the problems with the solution stability at a preset laminar boundary layer reflect the actual physical flow instability. So, RANS solution with the preset laminar boundary layer shows instability and, as a consequence, rising of the separation zone,

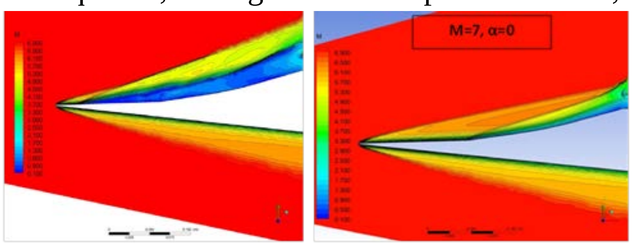

Laminar boundary layer, f≈0.5 | Turbulent boundary layer, f=0.95

FLUENT, M=7, α=0

Fig. 13. Mach number fields: FLUENT results with laminar (left) and turbulent (right) boundary layer.

which comes to the intake entrance and worsen its performance.

Fig. 13 shows the flow fields in the symmetry plane, obtained numerically by FLUENT with setting turbulent (right part of the figure), and laminar (left part of the figure) boundary layer at M_∞=7 and α=0°. It shows the Mach numbers fields in the symmetry plane. As you can see in Fig. 13, in the case of a turbulent boundary layer only a small local subsonic separation zone occurs on the intake surface. It covers not more than 30% of the entrance section. In the case of the laminar boundary layer, the large separation subsonic zone is visible, which extends downstream and covers almost whole entrance section.

Schlieren photography taken during the tests in the T-116 in the same mode is shown in lower picture of Fig. 14. It’s worth noting that the intake model was installed in the inverse position during the test campaign. The flow

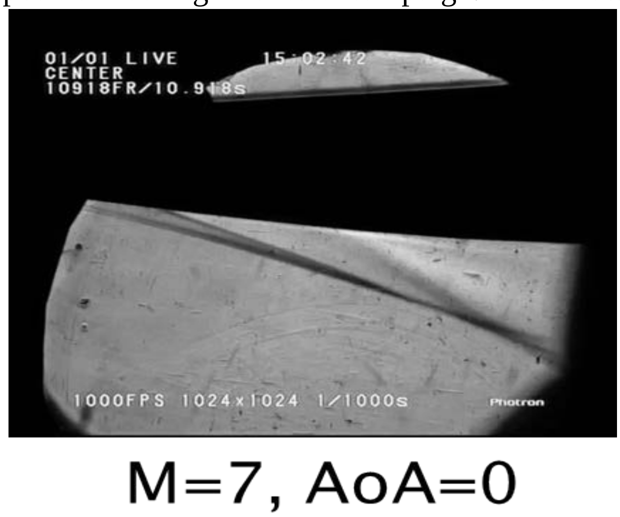

Fig. 14. Schlieren photography of the intake flow obtained in T-116 at M_∞= 7.

pattern on this photo is close to that obtained by numerical simulation with a predetermined laminar boundary layer, which confirms the above assumption about the nature of the flow on the intake compression surface.

Comparison of data on the intake air mass flow coefficient resulting from numerical simulations with preset turbulent and laminar boundary layer and the experimental data in the T-116 is shown in Fig. 15. The calculations with preset laminar boundary layer by package FLUENT, give significantly lower values of the

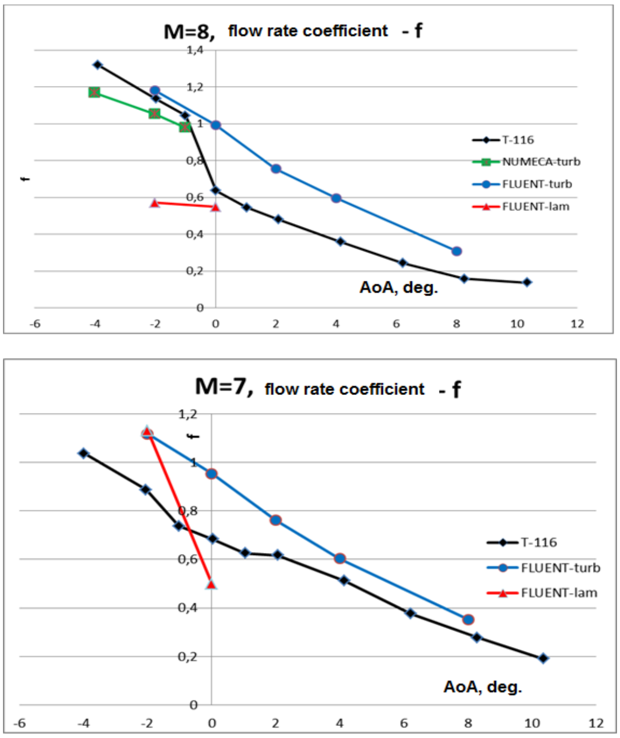

Fig. 15. Flow coefficient, FLUENT results with pre-determined turbulent and laminar boundary layer, M_∞= 7, 8.

intake air mass flow coefficient ≈ 0.5 ÷ 0.6, which is much closer to the experimental data.

Thus, the second series of calculations with laminar BL showed the development of a large separation zone, which covers most of the entrance to the engine duct, and, as a consequence, a significant degradation of the intake characteristics (unstart).

4.5 2nd series of tests in T-116

Analysis of the results of calculations and testing in a T-116 suggested that a significantly lower characteristics of this intake obtained in the experiment in comparison with the data of calculations with turbulent BL may result from the state of boundary layer at the intake compression surface (laminar boundary layer instead of a turbulent). Therefore, we can assume an increase in the intake air mass flow rate without substantial redevelopment of compression surface by the use of vortex generators. However, the shapes and forms of the turbulence generators, and the feasibility of their application require further engineering and scientific study.

2nd series of the test was conducted in T-116 to verify the assumptions about the influence of the nature of the flow in the boundary layer at the compression surface on the air intake characteristics. The same EFTV model was tested with the turbulence generators installed on the intake compression surface. When selecting the shape and location of the turbulence generators we took into account the results of the studies presented in [8].

The aim of the tests in the T-116 was to investigate the validity of the assumption that the strong degradation of the intake characteristics (unstart) is caused by the BL state on the compression surface, as well as the extent to which the turbulence generators can improve the intake start. The turbulence generators (Fig. 16) were produced in the form

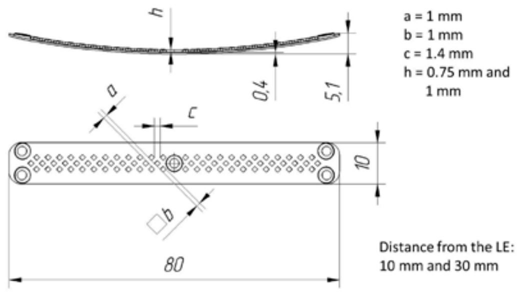

Fig 16. The turbulence generators for installation in the EFTV intake for tests in T-116.

of thin curved plates with a width of 10 mm, fitting for installation on the intake compression surface. The diamond-shaped roughness elements, were disposed on each plate in 3 rows, as shown on Fig. 16. The height of roughness elements was 1 mm and the plates were set at distances of 10 mm and 30 mm from the intake leading edge.

First tests of the model with the turbulence generators gave the negative result: the intake unstarted on all test regimes. It can be seen on Fig. 18, where the red line corresponds to the intake flow rate coefficients without turbulence generators, and the blue line – to the intake with turbulence generators plates (with BL tripping, var. 1). When the intake flow rate coefficient is about 1, it corresponds to the intake start. Without turbulence generators the start was observed at M=8 and negative AoA only. But the installation of turbulence generators plates leads to the intake unstart in whole range of regimes (blue line lower then 0.6 everywhere). At M=7 the situation is even worse.

We assumed that the plate with turbulence generators mounted on the surface after leading edge (Fig.17 Var. 1) creates small step, sufficient to initiate the shock wave, which reconstructs the whole flow picture. Therefore we decided to try various turbulence generators, shown on Fig.17:

1. Variant 1: two curved plates with roughness elements, shown on Fig. 16.
2. Variant 2: remove the plate as possible shock wave generator, and keep just 10 screws, which fixed the plates in Var. 1.
3. Variant 3: strain the wire between 10 screws obliquely in the form of X crosses.
4. Variant 4: strain the wire between 10 screws parallel to the leading edge.

Fig. 17. EFTV model in T-116 and the turbulence generator variants.

Black line on Fig. 18 presents the results of Var. 2. It is evident that 10 screws improve essentially the intake performances and provide the intake start at α=-4°÷2° and M=8. Fig. 18 demonstrates the flow rate coefficients for Variants 2, 3 and 4 at M=7. It shows that the intake start is also provided up to positive AoA. Let us notice that the wire addition to screws (Variants 3 and 4) does not change the result considerably.

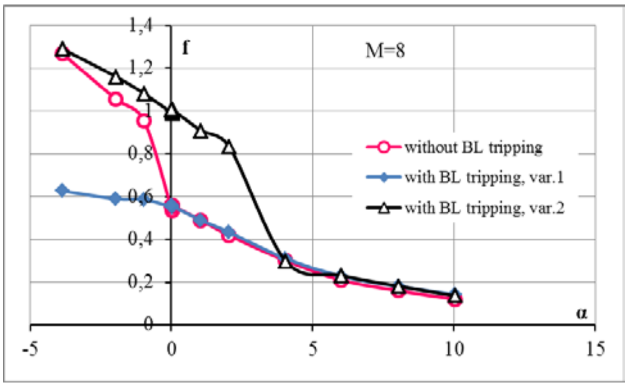

Fig. 18. Results of various turbulence generators.

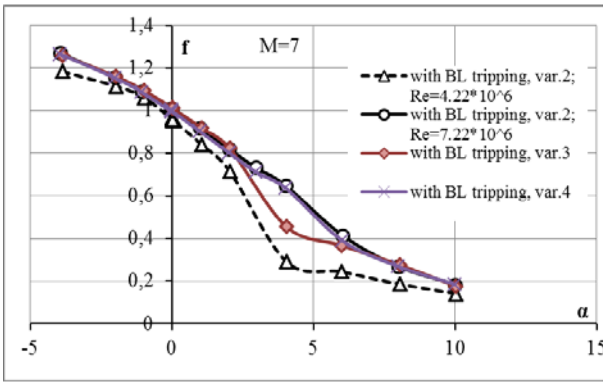

Fig. 19. Results of various turbulence generators.

The temperature measurements have been performed in the number of points on the EFTV model surface (see Fig. 20) to make sure of the BL state. The temperature measured in 17 points in the symmetry plane, 14 of them located on the bottom and 3 – on the top surface that is on the intake braking surface. Using temperature values we determined the temperature gradient and Stanton number – St_δ. Fig. 21 shows St_δ dependence on Re when BL is laminar (lower line) and turbulent (upper line). These curves are obtained on the basis of numerous tests in T-116. Apparently St_δ for turbulent BL is several times as many as for laminar one. It makes possible to determine the BL state using St_δ value. It seems on Fig. 20, BL on the bottom surface is laminar at M=7, and on the top surface BL is laminar in points 1 and 2, point 3 is in transition zone. As a result of the tripping elements installation (Var. 2-4) third point (№17) becomes in turbulent BL. Analogous results are obtained for M= 6 and 8. So, the measurements confirmed our assumptions concerning BL state.

Thus, as a result of proper selection of the turbulence generators we received significant improvement of the intake characteristics and the intake start on main regimes. The assumption that the cause of the discrepancy of calculation and experimental data is rooted in the wrong simulation of flow in the boundary layer is fully confirmed. The explanation of this phenomenon is based on the energy conservation law: in a turbulent flow occurs substantially larger energy dissipation than in a laminar one. So, when the BL flow is turbulent, the separation zone, formed in the central part of the flow region is substantially less and have less energy. In laminar BL after the surface break a powerful separation zone is generated, where due to the side cross-flows comes high-energy stream. This leads to an increase and enhancement of the separation zone, which eventually covers the entrance to the engine duct. The turbulence generators in this case act as the wave breakers.

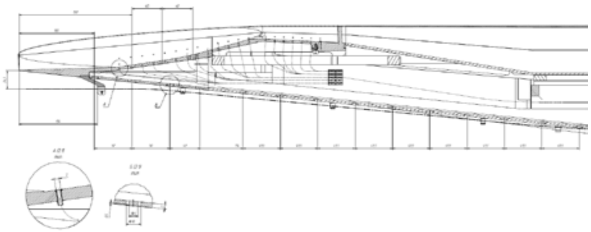

Fig. 20. Temperature measurements.

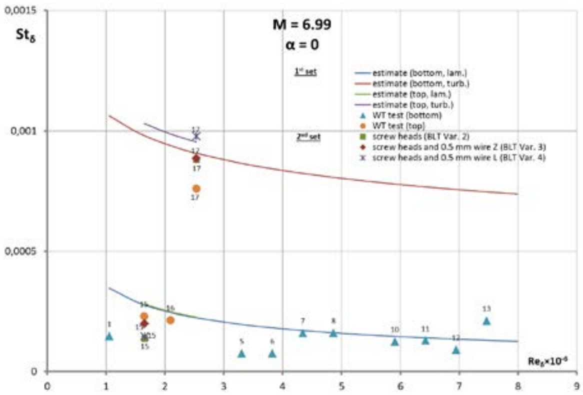

Fig. 21. BL state studies by Stanton number.

Conducted computational and experimental studies of the flow in the area of the air intake of high-speed aircraft model HEXAFLY-INT found that its main problem is the occurrence of subsonic separation zone in the central part of flow. This zone is developing downstream and reaches the entrance to the engine duct. It significantly worsens the intake characteristics until its unstart.

However, the state of the boundary layer on the intake compression surface has a decisive influence on the development of the separation zone downstream. The turbulent boundary layer in this case is more advantageous than the laminar one, since it is more stable. The BL turbulization has significantly improved the air intake performances, but the subsonic zone had not removed completely from the duct entrance, though it becomes smaller and weaker (it takes about 30% of the entrance area). The development of the duct flow and its interaction with this subsonic zone can lead to additional problems and require a separate careful investigation.

The EFTV vehicle of approximately 3m length is a scaled-down version of a potential passenger vehicle. Despite the considered Reynolds number is representative for the actual flight test conditions of the EFTV, the Re-number along the intake is considerably smaller than on the large-scale passenger vehicle. Hence, the transition point of the boundary layer will be relatively further downstream on this small scale model than on a large scale. One could be sure that the more stable turbulent state of the boundary layer is representative to the final passenger vehicle.

6 Conclusions

The numerical simulation and experimental studies of the flow in the air intake device of the high-speed civil aircraft model HEXAFLY-INT have been performed.

Conducted CFD and EFD studies of the flow in the area of the air intake of high-speed aircraft model HEXAFLY-INT have shown that its main problem is the occurrence of subsonic separation zone in the central part of flow in this intake.

However, the state of the boundary layer on the intake braking surface has a decisive influence on the development of the separation zone downstream. The turbulent boundary layer in this case is more preferable than laminar one, since it is more stable.

Right selection of the turbulence generators has resulted in significant improvement of the intake characteristics and the intake start on main regimes.

Acknowledgements

This work was performed within the ‘High Speed Experimental Fly Vehicles - International’ (HEXAFLY-INT) project fostering International Cooperation on Civil High-Speed Air Transport Research. HEXAFLY-INT, coordinated by ESA-ESTEC, is supported by the EU within the 7th Framework Program Theme 7 Transport, Contract no.: ACP3-GA-2014-620327. The project is also supported by the Ministry of Industry and Trade, Russian Federation. Further information on HEXAFLY-INT can be found on http://www.esa.int/techresources/hexafly_int.

References

[1] Steelant, J., Langener, T., Di Matteo, F., Hannemann, K., Riehmer, J., Kuhn, M., Dittert, C., Scheuerpflug, F., Jung, W., Marini, M., Pezzella, G., Cicala, M., Serre, L., “Conceptual Design of the High-Speed Propelled Experimental Flight Test Vehicle HEXAFLY”, 20th AIAA International Space Planes and Hypersonic Systems and Technologies Conference, Glasgow, Scotland, 6-9 July 2015: AIAA-2015-3539.

[2] Steelant, J., Varvill, R., Defoort, S., Hannemann, K., and Marini, M., “Achievements Obtained for Sustained Hypersonic Flight within the LAPCAT-II project”, 20th AIAA International Space Planes and Hypersonic Systems and Technologies Conference, Glasgow, Scotland, July 6-9, 2015: AIAA-2015-3677.

[3] Steelant, J. and Langener, T.: “The LAPCAT-MR2 hypersonic cruiser concept”, in 29th Congress of the International Council of the Aeronautical Sciences (ICAS), St. Petersburg, September 7 – 12, 2014.

[4] Meerts, C. and Steelant, J.: “Air Intake Design for the Acceleration Propulsion Unit of the LAPCAT-MR2 Hypersonic Aircraft”, in 5th European Conference for Aeronautics and Space Sciences (EUCASS), Munich, July 1 – 5, 2013.

[5] Billig F.S., Baurle R.A., Tam C.J. and Wornom S.F., ”Design and Analysis of Streamline Traced Hypersonic Intakes,”.*AIAA Paper* 1999-4974, 1999

[6] Karl, S. and Steelant, J.: “Cross-Flow Phenomena in Streamline Traced Hypersonic Intakes”, 20th AIAA International Space Planes and Hypersonic Systems and Technologies Conference, Glasgow, Scotland, 6-9 July 2015: AIAA-2015-3594.

[7] Voevodenko, N., Gubanov, A., Ivaniushkin, D., Lunin, V., Gusev, D., Ivankin, M., Talyzin, V.,

Yakovleva V., "Numerical and Experimental Studies of the Flow on HEXAFLY-INT Experimental Flight Test Vehicle Air Intake", 20th AIAA International Space Planes and Hypersonic Systems and Technologies Conference, Glasgow, Scotland, 6-9 July 2015: AIAA 2015-3584.

[8] Reda, D.C. "Review and Synthesis of Roughness-Dominated Transition Correlation for Reentry Applications". Journal of Spacecraft and Rockets, vol. 39, issue 2, pp. 161-167, 2002.

Contact Author Email Address

The contact author is Nina Voevodenko, TsAGI, whose e-mail is nina.voevodenko@tsagi.ru .

Copyright Statement

The authors confirm that they, and/or their company or organization, hold copyright on all of the original material included in this paper. The authors also confirm that they have obtained permission, from the copyright holder of any third party material included in this paper, to publish it as part of their paper. The authors confirm that they give permission, or have obtained permission from the copyright holder of this paper, for the publication and distribution of this paper as part of the ICAS proceedings or as individual off-prints from the proceedings.